Development 136, 1083-1092 (2009) doi:10.1242/dev.023820

Noncanonical frizzled signaling regulates cell polarity of growth plate chondrocytes

Yuwei Li and Andrew T. Dudley*

Bone growth is driven by cell proliferation and the subsequent hypertrophy of chondrocytes arranged in columns of discoid cells that resemble stacks of coins. However, the molecular mechanisms that direct column formation and the importance of columnar organization to bone morphogenesis are not known. Here, we show in chick that discoid proliferative chondrocytes orient the division plane to generate daughter cells that are initially displaced laterally and then intercalate into the column. Downregulation of frizzled (Fzd) signaling alters the dimensions of long bones and produces cell-autonomous changes in proliferative chondrocyte organization characterized by arbitrary division planes and altered cell stacking. These defects are phenocopied by disruption of noncanonical effector pathways but not by inhibitors of canonical Fzd signaling. These findings demonstrate that the regulation of cell polarity and cell arrangement by noncanonical Fzd signaling plays important roles in generating the unique morphological characteristics that shape individual cartilage elements.

KEY WORDS: Fzd signaling, Polarity, Chondrocyte, Planar cell polarity, Morphogenesis, Skeleton

INTRODUCTION

The growth of long bones is controlled via regulation of chondrocyte maturation in the growth plate cartilage, which is composed of four morphologically distinct zones of cells (see Fig. 1A-C) (Kronenberg, 2003). Resting chondrocytes comprise a population of progenitor cells that reside at the ends of the bones and exhibit a low level of cell cycle activation. Maturation begins with the formation of discoid proliferative chondrocytes that display increased cell cycle activity. After many rounds of division, the cell cycle is downregulated and the cells change shape (prehypertrophic chondrocytes). Subsequently, prehypertrophic chondrocytes enlarge to form hypertrophic chondrocytes that secrete the extracellular matrix protein collagen X and undergo cell death. Thus, the rate of long-bone growth is regulated via changes in cell number and cell volume (Breur et al., 1991; Hunziker et al., 1987).

The acquisition of unique morphogenetic properties is one remarkable characteristic of the maturation of resting chondrocytes into proliferative chondrocytes (Dodds, 1930). During the transition, individual resting chondrocytes, which are round and dispersed in the cartilage matrix, give rise to large single columns of tightly packed discoid proliferative chondrocytes. Whether the precise arrangement of chondrocytes depends on physical or mechanical properties of the extracellular environment (Aszodi et al., 2003; Ham, 1932), or is regulated by secreted signaling molecules (Abad et al., 2002), is unknown. Here we show that proliferative chondrocytes undergo oriented cell divisions that occur orthogonal to the direction of growth and then intercalate to form columns in a process that appears highly similar to convergent extension by cell intercalation (Keller et al., 1989; Keller et al., 2000). Both the division plane and cell orientation depend on noncanonical frizzled (Fzd) signaling. Disruption of Fzd signaling additionally alters polarized growth of the long bones, resulting in skeletal elements that are shorter and wider than wild-type bones. Together, these results suggest a model in which regulation of cell polarity by noncanonical Fzd signaling plays a crucial role in controlling the three-dimensional morphogenesis of skeletal elements.

Department of Biochemistry, Molecular Biology and Cell Biology, Northwestern University, 2205 Tech Drive, Evanston, IL 60208, USA.

*Author for correspondence (e-mail: a-dudley@northwestern.edu)

Accepted 28 January 2009

MATERIALS AND METHODS

cDNA preparation

Total RNA was isolated from stage-25 chick embryos or from the growth plate cartilage of E16 chick femora dissected free of the periosteum, using Trizol (Invitrogen) as per the manufacturer's instructions. RNA was treated with DNase I then reverse transcribed using Superscript III (Invitrogen). A control sample was prepared in parallel by omitting reverse transcriptase (–RT).

Construction of recombinant retrovirus

Retrovirus constructs were generated in RCAS(A) (Hughes, 2004) using the Slax21 shuttle vector and standard methods (Logan and Tabin, 1998). *Fzd7* and *dnFzd7* were subcloned as previously described (Hartmann and Tabin, 2000). Other sequences were amplified from stage-25 chick embryo cDNA by PCR (reaction details and primer sequences are available upon request). RCAS-*Dkk*, and RCAS-*dnLef1* and RCAS-*daCamKII* were gifts from C. M. Chuong (University of Southern California) and C. J. Tabin (Harvard Medical School), respectively. RISAP and RCAS(A)-daβ-catenin were provided by C. L. Cepko (Harvard Medical School) and Matsuhiro Iwamoto (Thomas Jefferson University College of Medicine), respectively. Concentrated virus stocks (10^8-10^9 pfu/ml) were prepared by standard procedures (Logan and Tabin, 1998), except for RISAP, RCAS(A)-D2, RCAS(A)-$D2^{KM}$ and RCAS(A)-dnRock, which were pseudotyped with VSV-G and produced by transient expression to 10^6-10^7 pfu/ml (Chen et al., 1999).

Processing of chick embryos

Fertilized chicken eggs (Phil's Fresh Eggs, Forreston, IL, USA) were grown at 37.5°C and staged (HH) as described (Hamburger and Hamilton, 1992). Concentrated retrovirus stocks were injected into the right forelimb at HH 19-21. For mosaic analysis, stocks were diluted to 10^7 pfu/ml in DMEM+0.1% FBS. After incubation, the humerus and ulna were dissected and fixed in 4% paraformaldehyde in PBS (pH 7.2) at 4°C. Micromass cultures were prepared and analyzed as described (Cottrill et al., 1987; Tufan et al., 2002).

Histology

To analyze cell morphology, tissue was fixed overnight, dehydrated through an ethanol series, embedded in paraffin (Paraplast X-tra, Tyco-Healthcare) and sectioned. Hematoxylin and Eosin (H&E) staining was performed using

a standard protocol. For quantification of bone dimensions, the length and width (halfway between the articular surface and the mineralized region) were determined from the center section of a cartilage element (n=4 for each condition). For lineage analysis, harvested tissue was fixed for 4 hours, washed in PBS, heat-inactivated at 65°C for 30 minutes, and stained for alkaline phosphatase activity as described (Chen et al., 1999).

To analyze cell proliferation, S-phase cells were labeled with the nucleotide analog bromodeoxyuridine (BrdU) for 4 hours prior to tissue harvest. Sections of BrdU-labeled tissue were digested in trypsin and depurinated in hydrochloric acid. Incorporated BrdU was detected using a mouse anti-BrdU monoclonal antibody (G3G4, S. J. Kaufman, Developmental Studies Hybridoma Bank, Iowa, USA) and Cy2-labeled donkey anti-mouse antibody (Jackson ImmunoResearch, Pennsylvania, USA). Nuclei were counterstained with 4′,6-diamidino-2-phenylindole (DAPI; Sigma-Aldrich). The BrdU labeling index was calculated as the percentage of total nuclei (DAPI-stained) that were BrdU-positive.

Gene expression analysis

Transcripts of Fzd pathway components were detected by PCR (reaction details and primer sequences are available upon request). Whole-embryo RNA from pools of HH 16-23 chick embryos was used as a positive control (data not shown). Bands were visible on ethidium bromide-stained agarose gels after 27-29 cycles, whereas background bands in –RT samples were only observed after more than 35 cycles. For in situ hybridization analysis, tissue sections were hybridized to RNA probes labeled with digoxigenin (Roche) as described (http://genepath.med.harvard.edu/~cepko/protocol).

Analysis of cell division orientation and cell arrangement

We adapted previously described methods to analyze cell division in sections of fixed tissue (Gong et al., 2004; Tibber et al., 2004). Dissected cartilage was fixed overnight, equilibrated in 30% sucrose in PBS, and frozen in O.C.T. Compound (Tissue-Tek). Tissue was cryosectioned at 20 μm, mounted on Superfrost Plus slides (VWR), and briefly air-dried. Sections were washed in PBS, permeabilized in 1% Triton X-100, and incubated with rhodamine-phalloidin (1:100; Molecular Probes) and DAPI (0.1 μg/ml; Sigma) to label the contractile ring and DNA, respectively. Three-dimensional images were generated from a z-series of optical sections collected on a Zeiss apotome deconvolution microscope. The orientation of cell division was determined by mathematical modeling in which a cube was drawn with daughter nuclei occupying diagonal corners on opposite faces (see Fig. 2D). In this model, line segment ‘b’ is set parallel to the long axis of the cartilage (equivalent to the distance between the nuclei in the y-axis) and line segment ‘a’ is the distance between nuclei in the x-axis. Line segments ‘a’ and ‘b’ were measured using Zeiss Axiovision software. Line segment ‘c’ (the distance between daughter nuclei in the z-axis) was determined by counting the number of 1 μm optical sections spanning the centers of the daughter nuclei. The angle (θ) generated by the intersection of line segment ‘b’ and a line segment connecting the daughter nuclei was determined using the formula shown in Fig. 2D. Calculated angles were categorized into bins of 10° and the percentage of the total cells in each bin was plotted as a bar chart. Cells in metaphase were imaged using anti-γ-tubulin (1:1500; Sigma), secondary anti-mouse Cy3 (1:500; Jackson ImmunoResearch) and DAPI (0.1 μg/ml). Spindle orientation at metaphase was calculated by applying the same mathematical model as above except that the cube was drawn with apposing centrosomes at opposite corners.

The orientation of the long axis of the cell was determined from section in situ hybridizations. θ_{cell} is defined by the intersection of a line drawn through the longitudinal axis of the cell profile and a line drawn parallel to the long axis of the cartilage.

Statistical methods

Data for each manipulation were obtained from at least six limbs (a minimum of three limbs on each of two days) except where noted in the text and see Table S1 in the supplementary material. The Kolmogorov-Smirnov test was used to determine whether the distributions of θ were distinct for different experimental conditions (Herrick, 1965; Ong and LeClare, 1968). For this analysis, P>0.05 demonstrates similarity between compared distributions. Tests for arbitrary angles compared the observed values to a uniform distribution over θ=0-90°.

RESULTS

Proliferative chondrocytes display stereotypical cell behaviors

Columns of discoid proliferative chondrocytes are readily observed late in embryogenesis because thick extracellular matrix separates individual stacks of cells (Dodds, 1930). To determine whether the unique organization of proliferative chondrocytes depends on physical restriction by the extracellular matrix, we examined cell behavior in chick long bones at early developmental stages. At embryonic day 9 (E9; HH 33-35), proliferative chondrocytes are elongated but not organized into obvious columns (Fig. 1C). However, progeny of individual chondroprogenitor cells labeled by infection with the replication-defective avian retrovirus, RISAP (Chen et al., 1999), displayed a zone-specific arrangement. Thus, resting chondrocytes gave rise to clones displaying radial symmetry (25/25) (Fig. 1D), whereas 80% of clones (39/48) in the proliferating zone formed single columns (Fig. 1E). A minority of clones (data not shown) appeared either as two adjacent columns (7/48) or as large groups of labeled cells (2/48). Thus, columnar organization is an intrinsic behavior of proliferative chondrocyte clones at all stages of development.

Although columns of proliferative chondrocytes grow by clonal expansion, cell division is biased against orientations that result in daughter cells aligned parallel to the column (Dodds, 1930). We asked whether the division plane, like column organization, is regulated prior to the thickening of the extracellular matrix. In sections of E9 long bones (Fig. 2B), cells in telophase were identified by the presence of an actin-rich contractile ring between two future daughter cells (Fig. 2C,E). An angle of cell division, termed θ, was determined from three-dimensional images (Fig. 2D) (see Materials and methods), such that 0° defines a cleavage plane that generates daughter cells arranged in a column, and 90° divisions displace daughters laterally with respect to the forming column. Wild-type resting chondrocytes divided at arbitrary angles, whereas wild-type and GFP-expressing proliferative chondrocytes exhibited a strong bias for telophase θ=81-90° (Fig. 2F; see Fig. S1 in the supplementary material). Bias in telophase θ was observed in E6 (HH 27) (Fig. 2A,F) proliferative chondrocytes and in E9 prehypertrophic chondrocytes (Fig. 2F). Thus, collectively, and consistent with our lineage data, resting and proliferative chondrocytes display distinct behaviors that remain substantially unaffected by developmental changes in the microenvironment.

What, then, restricts the plane of division in proliferative chondrocytes? One possibility consistent with Hertwig’s Rule (Wilson, 1900) is that the discoid cell shape constrains the mitotic apparatus to lateral orientations (Carreira-Barbosa et al., 2003; Toyoshima and Nishida, 2007). If this is the case in proliferative chondrocytes, orientation of the mitotic spindle at metaphase (Fig. 2G) should be similar to telophase θ. Unexpectedly, metaphase θ (Fig. 2H) was significantly different from telophase θ (Fig. 2F) (P<0.0001), demonstrating that spindle formation is not restricted to a specific axis. Furthermore, metaphase θ was highly similar in the morphologically distinct resting and proliferative chondrocytes (Fig. 2H) (P=0.555), indicating that the position at which the spindle forms is not strongly influenced by chondrocyte shape.

Decreased Fzd signaling interferes with oriented cell divisions

Spindle rotation during asymmetric cell divisions in *Drosophila* (Adler and Taylor, 2001; Roegiers et al., 2001) and in *Caenorhabditis elegans* (Wu and Herman, 2006a) requires *Fzd* function. Although Fzd signaling is important for growth plate

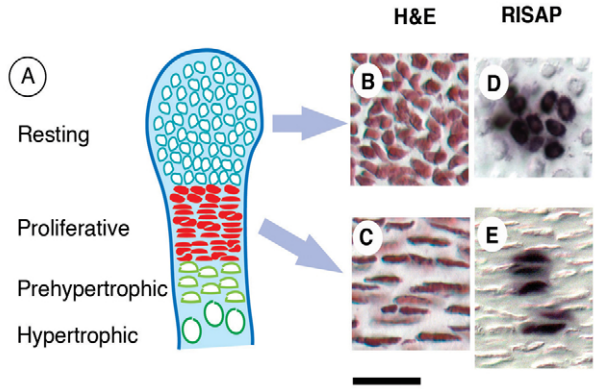

Fig. 1. Resting and proliferative chondrocytes display distinct behaviors. (**A**) The growth plate contains distinct zones composed of resting, proliferative, prehypertrophic and hypertrophic chondrocytes. (**B**,**C**) H&E-stained paraffin sections of E9 chick cartilage reveal the transition from round disordered cells to ordered discoid cells that accompanies the maturation of resting chondrocytes (B) into proliferative chondrocytes (C). (**D**,**E**) To determine the relationship between clonal expansion and tissue structure, E3 limb buds were injected with RISAP virus, incubated to E9, and stained for alkaline phosphatase activity (purple). Resting chondrocytes give rise to clones that expand with radial symmetry (D). By contrast, proliferative chondrocyte clones form columns (E). Scale bar: 50 μm in B-E.

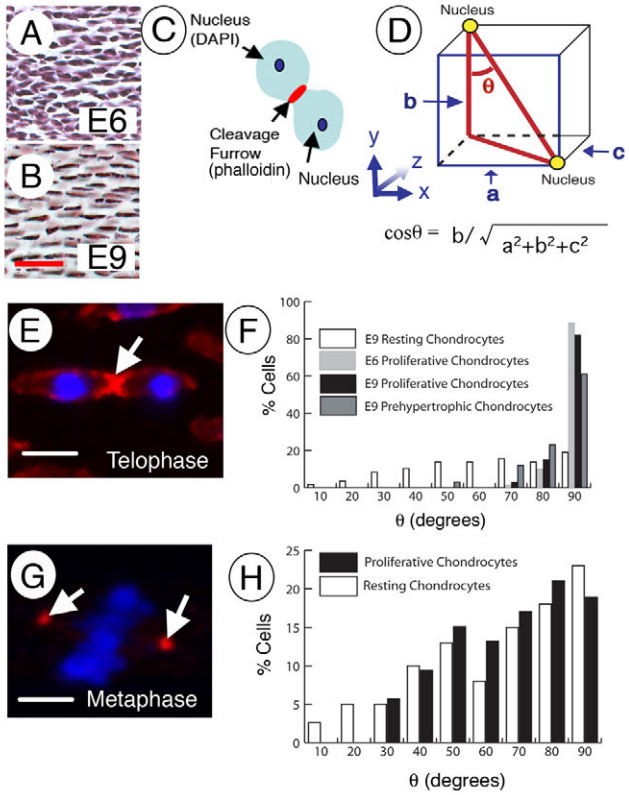

Fig. 2. Oriented cell divisions in proliferative chondrocytes. (**A**,**B**) The structure of the proliferative zone changes as chick cartilage matures between E6 and E9 from a dense packing to an ordered array of individual cells. (**C**,**E**) To test whether order in the proliferative chondrocytes involves oriented cell divisions, the plane of cell division was visualized in tissue sections using DAPI to label the nuclei and rhodamine-phalloidin to label the cleavage furrow or contractile ring (arrow in E). (**D**) The orientation of cell division (θ) relative to the long axis of the cartilage (parallel to 'b') was calculated from measurements obtained from 3D images of cells in telophase using the equation provided (see Materials and methods for details). (**F**) This method revealed that resting chondrocyte progenitors divide at arbitrary angles that are nonuniformly distributed ($P<0.005$), whereas proliferative chondrocytes and prehypertrophic chondrocytes display divisions aligned at θ=81-90° (distinct from resting cells at $P<0.0001$). Aligned planes of cell division are characteristic of proliferative chondrocytes as early as E6 ($P<0.0001$ versus resting cells). (**G**) Orientation of the mitotic spindle at metaphase was determined by a similar method, except that the hypotenuse in D is a line that connects the two γ-tubulin containing centrosomes (arrows) flanking condensed chromatin (blue) at the metaphase plate. (**H**) When assessed by this method, resting and proliferative chondrocytes display similar distributions of θ at metaphase ($P=0.555$). Scale bars: 25 μm in B for A,B; 6.4 μm in E; 3 μm in G.

function (Hartmann and Tabin, 2000), a role for *Fzd* in regulating the division plane in chondrocytes has not been reported. To test this possibility, we used replication-competent avian retrovirus (RCAS) (Hughes, 2004) to express a C-terminal truncated form of chicken frizzled 7 (Fzd7^{-C}) (Hartmann and Tabin, 2000) in the chick forelimb. Chicken Fzd7^{-C} is analogous to a molecule that inhibits Fzd signaling by a dominant-negative mechanism in zebrafish (Nasevicius et al., 1998). E9 humeri uniformly expressing high levels of *Fzd7^{-C}* are significantly shorter and wider than those of uninfected controls (Fig. 3A,C), but cell proliferation was not affected (Fig. 4). In these limbs, infected resting chondrocytes appeared normal (Fig. 4C), whereas proliferative chondrocytes displayed aberrant cell morphology and the long cell axes were not aligned (Fig. 4I). Nonetheless, infected cells flattened at a position consistent with the normal interface between resting chondrocytes and proliferative chondrocytes (data not shown), suggesting that downregulation of Fzd signaling neither interferes with cell morphology in general, nor disrupts global organization of the growth plate.

To test whether the observed abnormalities reflect failed chondrocyte maturation, we examined the expression of specific genes (see Fig. S2 in the supplementary material). *Fzd7^{-C}*-expressing chondrocytes appropriately express early chondrocyte collagens (*Col2a1* and *Col9a1*) and do not express collagen I (*Col1a1*), which is produced by dedifferentiated chondrocytes, osteoblasts and other mesenchymal cells. In addition, infected cartilage contains domains of Indian hedgehog (*Ihh*)-expressing prehypertrophic chondrocytes that surround a central region of hypertrophic cells (Fig. 4; see Fig. S2 in the supplementary material). These domains of mature chondrocytes are greatly reduced in size compared with wild-type cartilage, as previously described (see Fig. S2 in the supplementary material) (Hartmann and Tabin, 2000). Although *Ihh* expression is decreased, *Fzd7^{-C}*-expressing resting and proliferative chondrocytes express parathyroid hormone related peptide (*Pthlh*) and patched (*Ptch*), respectively (Hartmann and Tabin, 2000). *Pthlh* and *Ptch* are two Ihh-responsive genes that are also components of a key feedback loop that regulates proliferative chondrocyte formation (reviewed by Kronenberg, 2003; Yang et al., 2003). Together, these data suggest that chondrocytes expressing *Fzd7^{-C}* undergo maturation and participate in long-range signaling interactions between the resting and prehypertrophic chondrocytes that are crucial to maintain growth plate architecture and function.

We next examined the division plane in infected E9 chondrocytes. Expression of *Fzd7^{-C}* did not affect telophase θ of resting chondrocytes, whereas telophase θ for infected proliferative

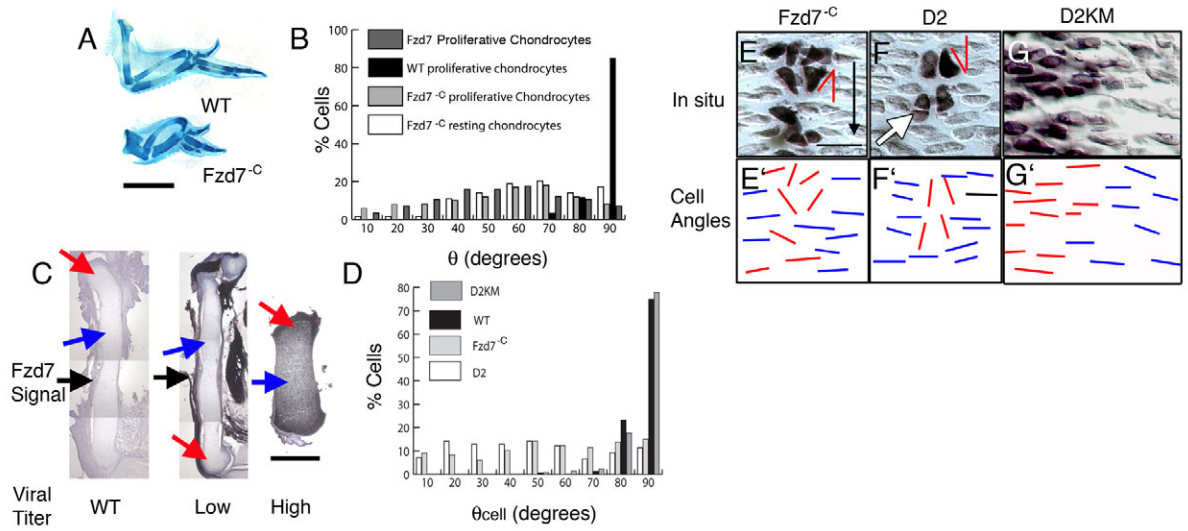

Fig. 3. Cell-autonomous Fzd signaling regulates the polarity of proliferative chondrocytes. (**A**) Infection of the chick limb with RCAS(A)-Fzd7^{-C} results in long bones that are shorter and wider than wild-type elements. Images oriented with the shoulder joint at the top. (**B**) Proliferative chondrocytes infected with RCAS(A)-Fzd7^{-C} display a uniform distribution of θ (P=0.133) that is distinct from that of uninfected (WT) cells (P<0.0001), whereas telophase θ for RCAS(A)-Fzd7^{-C}-infected resting chondroctyes is non-uniform (P<0.001) as in wild-type resting cells. Telophase θ of *Fzd7*-expressing proliferative chondrocytes is indistinguishable from that of cells expressing *Fzd7*$^{-C}$ (P=0.738). (**C**) Cartilage growth defects are dependent on infection of chondrocytes. Humeri from uninjected (WT) limbs, and limbs injected with low or high titer RCAS(A)-Fzd7^{-C} virus were mounted on the same slide and hybridized with a riboprobe complementary to chicken *Fzd7*. WT limbs show low levels of signal in the perichondrium (black arrow) but not in chondrocytes (red arrow). Injection of low titer virus results in a strong infection in the perichondrium and weak to no infection of the cartilage, with no discernable effect on cartilage length. High titer virus results in ubiquitous infection of the chondrocytes and produces growth defects that include shortening (689.0±124.4 μm versus 1494.0±165.3 μm in WT; n=4 humeri per condition) and widening (258.5±49.3 μm versus 137.5±12.8 μm in WT) of the humerus. (**E-G′**) Mosaic cartilage was generated by infection with low titer virus encoding *Fzd7*$^{-C}$, *D2* or *D2*^{KM}. Infected cells were detected by in situ hybridization for the mutant molecule expressed from the virus (purple) and visualized by differential interference contrast microscopy. The red wedges define an angle θ_{cell} that describes the relationship between the orientation of the long axis of the adjacent infected cell and the longitudinal axis of the cartilage (black arrow in E). E′-G′ are schematic representations of the orientation of the long axes of the wild-type (blue bars) and infected (red bars) cells in E-G. (E,E′) Disorder of *Fzd7*$^{-C}$-expressing proliferative chondrocytes is readily apparent by comparing the arrangement of small patches of infected cells with their wild-type neighbors (unstained cells). (F,F′) Similar effects are observed in cells expressing *D2* (note the abnormal cell division, which is nearly parallel to the long axis of the cartilage; white arrow), but not in cells expressing *D2*^{KM} (G,G′), which is deficient in blocking noncanonical Fzd signaling. (**D**) Quantitative image analysis (see E-G′) reveals that wild-type and D2^{KM} cells are aligned orthogonal to the cartilage axis, whereas θ_{cell} for chondrocytes expressing *Fzd7*$^{-C}$ or *D2* is uniformly distributed from 0-90° (P<0.001), demonstrating that inhibition of Fzd signaling results in cell-autonomous defects in chondrocyte polarity. Scale bars: 500 μm in A; 400 μm in C; 50 μm in E-G.

chondrocytes was uniformly distributed from 0-90° (P=0.133) (Fig. 3B). In agreement with previous studies that demonstrated similar phenotypes in limbs expressing *Fzd7*$^{-C}$ and wild-type *Fzd7* (Hartmann and Tabin, 2000), we found that *Fzd7* expression resulted in a telophase θ indistinguishable from that of *Fzd7*$^{-C}$-expressing proliferative chondrocytes (Fig. 3B) (P=0.738). Collectively, our data suggest that chondrocyte polarity is highly sensitive to Fzd signaling levels.

Cell-autonomous function of Fzd signaling

Cartilage growth is a tightly controlled process that involves interactions between chondrocytes and the perichondrium/periosteum (PC/PO) (Alvarez et al., 2001; Hinoi et al., 2006), a tissue that lines the developing cartilage. Thus, effects of *Fzd7/Fzd7*$^{-C}$ expression on chondrocyte morphogenesis might result from defects in PC/PO function. To test this possibility, we asked whether infection of the PC/PO is sufficient to produce the observed phenotype. This test is possible because we found that soft tissues of the limb, including the PC/PO, are more easily infected with replication-competent virus than cells of the cartilage. Thus, injection of lower titer virus stocks results in highly infected PC/PO and few infected chondrocytes (Fig. 3C; see Fig. S3 in the supplementary material). Moreover, these data demonstrate that in situ hybridization can be used to identify infected cells in tissue sections because the inserted sequence is expressed at higher levels than the endogenous locus. In this context, limbs infected with low titer virus are similar to wild-type limbs in cartilage length and chondrocyte morphology (Fig. 3C; see Fig. S3 in the supplementary material). These data strongly suggest that Fzd signaling in the PC/PO does not regulate growth plate architecture or the growth properties of cartilage elements.

We next asked whether the organization of the proliferative chondrocytes depends on cell-autonomous *Fzd* function. We created mosaic embryos by injecting diluted virus to generate small patches of infected chondrocytes surrounded by large numbers of wild-type cells. Cells within patches expressing *Fzd7*$^{-C}$ displayed a range of morphological defects, but most cells had clearly defined long and short axes (Fig. 3E). Quantification of cell orientation (θ_{cell}; see Materials and methods) revealed that wild-type cells adjacent to infected patches displayed normal orientation (Fig. 3D,E,E′). By contrast, expression of *Fzd7*$^{-C}$ randomized the cell orientation, even when infected chondrocytes

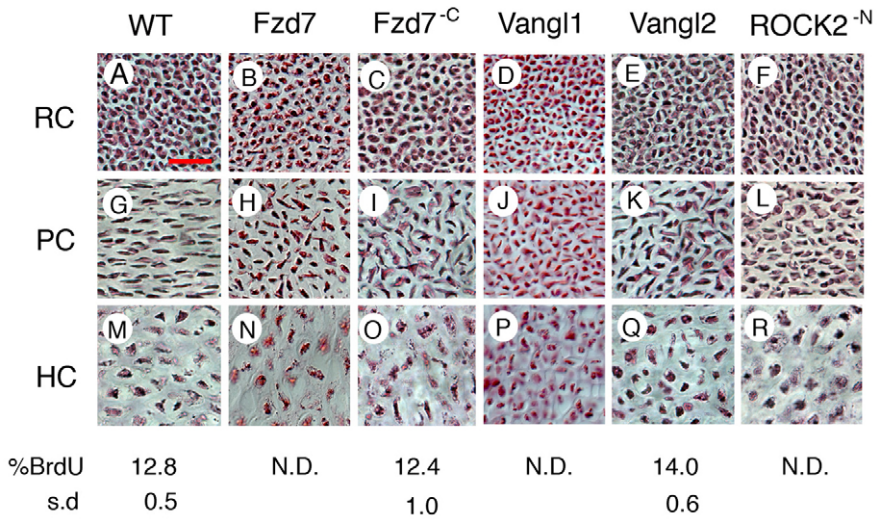

Fig. 4. Disruption of Fzd signaling alters the morphology of proliferative chondrocytes. Uninfected wild-type (WT) chick cartilage (**A**,**G**,**M**) and elements expressing *Fzd7* (**B**,**H**,**N**), *Fzd7*$^{-C}$ (**C**,**I**,**O**), *Vangl1* (**D**,**J**,**P**), *Vangl2* (**E**,**K**,**Q**) or Rock2^{-N} (**F**,**L**,**R**) were stained with H&E. Images of the resting chondrocytes (RC), proliferative chondrocytes (PC) and hypertrophic chondrocytes (HC) demonstrate that defects are first observed in the proliferative chondroctyes. Cell proliferation (%BrdU) is not affected by expression of *Fzd*$^{-C}$ or *Vangl2*. *n*=3 limbs per condition. N.D., not determined. Scale bar: 50 μm.

were surrounded by wild-type cells that displayed normal morphology (Fig. 3D,E,E′). To confirm that altered morphology results from cell-autonomous defects in Fzd function, we asked whether a similar phenotype would result from downregulation of dishevelled (Dsh, also known as Dvl), an intracellular signaling mediator that directly interacts with Fzd via a PDZ domain (Wallingford and Habas, 2005). PDZ-domain deletions of *Dsh* [D2 construct in Rothbacher et al. (Rothbacher et al., 2000)] abrogate Fzd signaling in a dominant-negative manner (Axelrod et al., 1998). Cells expressing D2 had a measurable long axis that was misaligned (Fig. 3D,F,F′). Thus, *Fzd* function autonomously regulates cell polarity and cell arrangement in the proliferative chondrocytes.

The orientation of cell division is not sensitive to levels of canonical Fzd signaling

Having demonstrated a role for Fzd signaling in chondrocyte polarity, we next asked which Fzd effector pathway is disrupted by *Fzd7*$^{-C}$ expression. The canonical Fzd pathway acts via stabilization of the transcriptional regulator β-catenin (Papkoff et al., 1996). To test whether reduced β-catenin function accounts for the observed defects in polarity, we expressed dickkopf 1 (*Dkk*) (Suksaweang et al., 2004), an extracellular antagonist that blocks activation of the β-catenin-dependent pathway, and a putative dominant-negative mutant form of *Lef1* (*dnLef1*) (Kengaku et al., 1998), a key component of the β-catenin transcriptional complex (Fig. 5A-C). Consistent with their predicted activities, expression of these inhibitory molecules enhanced cartilage formation in micromass cultures of chick limb mesenchyme (Fig. 5D). In vivo, chondrocytes expressing *dnLef1* and *Dkk* displayed minor morphological changes (Fig. 5B,C), but telophase θ was similar to that of wild-type proliferative chondrocytes (Fig. 5I). As a further test of the requirement to regulate β-catenin activity, we expressed a truncated form of β-catenin that lacks the N-terminal domain that confers instability and is therefore constitutively activated (daβ-cat) (Rubinfeld et al., 1997). In mosaic cartilage, groups of morphologically normal *daβ-cat*-expressing cells were readily observed in both resting and proliferative chondrocytes (Fig. 5F,G). Collectively, these data suggest that proliferative chondrocyte morphogenesis is not sensitive to β-catenin levels. Consistent with this, proliferative chondrocytes display normal organization in β-catenin mutant mice (Hill et al., 2005; Mak et al., 2006).

Noncanonical Fzd signaling regulates the plane of cell division

Since interfering with the canonical pathway did not alter the division plane, we next addressed whether the polarity defects observed in *Fzd7*$^{-C}$-expressing chondrocytes could result from altered noncanonical signaling. Gene expression analysis revealed the presence of multiple isoforms of calcium-calmodulin dependent protein kinase II (CamKII), which are components of the noncanonical Fzd/Ca^{2+} pathway in chick growth plate cartilage (Kuhl et al., 2000). Because putative dominant-negative forms of CamKII are weak inhibitors of the pathway, we tested the role of Fzd/Ca^{2+} signaling by ectopically expressing a constitutively active form of CamKIIα (daCamKII) (Abzhanov et al., 2006; Kuhl et al., 2000). Expression of daCamKII altered cell morphology (Fig. 5H) and shifted the plane of cell division from telophase θ=81-90° (Fig. 5I). These data are consistent with a potential role for noncanonical Fzd signaling in orienting the plane of cell division, but do not fully account for the uniform telophase θ in cells expressing *Fzd7*$^{-C}$.

Our gene expression analysis also showed that some components of the noncanonical planar cell polarity (PCP) pathway (Klein and Mlodzik, 2005) are expressed in the developing growth plate (Fig. 5J). The possibility that a PCP-like pathway functions in proliferative chondrocytes is further supported by the similar phenotypes in Fzd loss- and gain-of-function experiments (Fig. 3B) (Krasnow and Adler, 1994) and the fact that *D2* has a stronger inhibitory effect on the PCP pathway than on the β-catenin-dependent pathway (Axelrod et al., 1998; Krasnow and Adler, 1994; Rothbacher et al., 2000). Since PCP signaling requires the DEP domain in Dsh (Rothbacher et al., 2000; Wallingford and Harland, 2002; Wallingford et al., 2000), we first tested whether the effect of *D2* on cell orientation requires DEP function. We introduced a missense mutation into *D2* (K441M; *D2*^{KM}), analogous to the *dsh1* mutation in *Drosophila* that specifically abrogates DEP-dependent PCP signaling by *dishevelled* but permits normal activation of β-catenin-dependent signaling (Axelrod et al., 1998; Boutros et al., 1998). The K441M mutation blocked the ability of *D2* to interfere with chondrocyte morphogenesis (Fig. 3D,G,G′). These data suggest that *D2* function depends on interaction with effectors of PCP signaling.

In the *Drosophila* wing, localization of Van Gogh (Strabismus; vertebrate Vangl), a four-pass transmembrane regulator of PCP signaling that interacts with Dsh (Park and Moon, 2002), to the plasma membrane on one face of the cell confers polarity that aligns

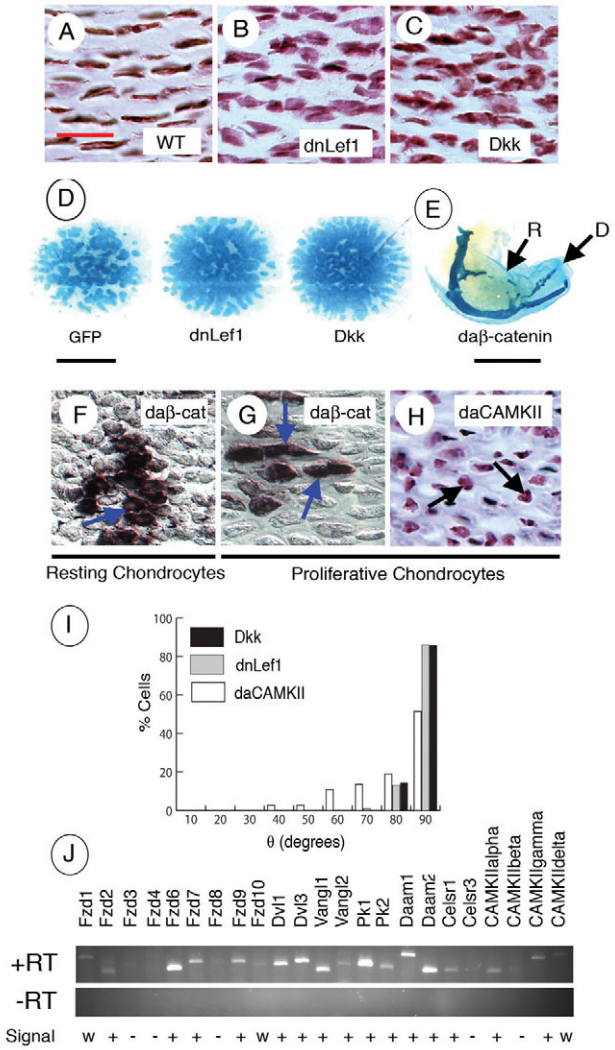

Fig. 5. The orientation of cell division in proliferative chondrocytes is insensitive to canonical Fzd signaling but is partly dependent on Wnt/Ca^{2+} signaling. (**A-C**) Paraffin sections of E9 chick long bones stained with H&E. Wild-type (WT) cells are discoid (A), whereas expression of the canonical pathway antagonists *dnLef1* (B) and *Dkk1* (C) results in cells that display abnormal morphology. (**D**,**E**) Controls for expressed protein activity. In micromass cultures, limb mesenchyme cells infected with RCAS(A)-GFP form numerous cartilage nodules (blue) that are similar in size and spacing. By contrast, expression of *dnLef1* or *Dkk* promotes increased chondrogenesis as determined by the decrease in spacing between individual nodules. (E) Widespread expression of a stabilized mutant of β-catenin, daβ-catenin, suppresses cartilage formation. Note the absence of the radius (R) and poor formation of the digits (D; compare with wild-type limbs in Fig. 3A). (**I**) Despite the change in shape, cell division in infected proliferative chondrocytes is indistinguishable from wild type (P=0.976 and 0.968 for *dnLef1* and *Dkk*, respectively). (**F**,**G**) Expression of daβ-catenin (daβ-cat; purple, arrows) does not alter the morphology of resting (n=25/25, 4 limbs) or proliferative (n=29/30, 4 limbs) chondrocytes. The arrows in G indicate infected proliferative chondrocytes dividing in the correct plane. (**H**) By contrast, constitutive activation of the Wnt/Ca^{2+} pathway by expression of activated *CamKIIa* (*daCamKII*) produces round cells (arrows) that display telophase θ (see I) that is distinct from both resting (P<0.001) and proliferative (P<0.001) chondroctyes. (**J**) Gene expression analysis was performed on Fzd signaling pathway core components [Fzd receptors and Dsh (Dvl)], PCP components (Vangl, Prickle/Pk, Daam and Celsr) and Ca^{2+} regulators (CamKII). cDNA synthesized from total growth plate RNA was analyzed by PCR (+RT) as described in Materials and methods (and see Table S1 in the supplementary material). Control samples using RNA not subjected to reverse transcription (–RT, negative control) and total cDNA from HH 25 embryos (positive control, not shown) were run in parallel. Signal was judged as present (+), weak (w) or absent (–) after 28-30 cycles based on analysis of ethidium bromide-stained agarose gels. Signal was detected in the –RT control after 38 cycles. Scale bars: in A, 50 μm for A-C,F,G and 100 μm for H; 2 mm in D,E.

hairs in the plane of the epithelium (Klein and Mlodzik, 2005). As such, both gain- and loss-of-function *Vangl* mutations disrupt PCP in *Drosophila* and vertebrates (Krasnow and Adler, 1994). We expressed chick *Vangl2* bearing a C-terminal hemagglutinin epitope tag ($Vangl2^{HA}$) in the wing cartilage and confirmed, by immunofluorescence, that the protein is secreted to the membrane (Fig. 6B,B′). Like $Fzd7^{-C}$, expression of *Vangl2* generated short, wide cartilage elements (Fig. 6A) containing disorganized proliferative chondrocytes (Fig. 4K) that displayed normal cell cycle characteristics (Fig. 4) but reduced zones of mature chondrocytes (see Fig. S2 in the supplementary material). Similar to $Fzd7^{-C}$, expression of *Vangl2* resulted in a uniform telophase θ (Fig. 6D) (P=0.103). Expression of the related gene, *Vangl1*, produced results indistinguishable from those of *Vangl2* by histology (Fig. 4J) and telophase θ (Fig. 6D) (P=0.75). In addition, *Vangl2* expression randomized the orientation of proliferative chondrocytes in a cell-autonomous manner (Fig. 6C,C′,E). Expression of a truncated form lacking the C-terminal PDZ-binding motif ($Vangl2^{-C}$) that is required for interaction with the PCP pathway but not the canonical pathway (Park and Moon, 2002), did not affect cartilage growth (Fig. 6A) or the division plane (Fig. 6D), suggesting that, as with *D2*, the effect of *Vangl2* expression is dependent on interaction with downstream effectors of the PCP pathway. Potential downstream effectors of this pathway include the Rho GTPases and Rho-associated kinase 2 (Rock2) (Kim and Han, 2005; Phillips et al., 2005). We determined the effect of altered Rho pathway function by expressing a putative dominant-negative fragment of chicken Rock2 ($Rock2^{-N}$) (Leung et al., 1996) in the developing wing. Expression of $Rock2^{-N}$ had a marked effect on proliferative chondrocytes, resulting in changes in cell morphology (Fig. 4L) and in the division plane (Fig. 6D) that were highly similar to those of chondrocytes expressing $Fzd7^{-C}$ and *Vangl2*. Collectively, these data suggest the possibility that the regulation of Rho by noncanonical Fzd signaling controls the plane of cell division and cell polarity in proliferative chondrocytes.

DISCUSSION

Fzd signaling regulates chondrocyte polarity

One remarkable characteristic of proliferative chondrocytes is the precise alignment of the cell division plane. In this process, spindle orientation at metaphase is refined to telophase θ=81-90° in proliferative chondrocytes, but remains unrefined in resting chondrocytes. Collectively, our data suggest that noncanonical (β-catenin-independent) Fzd signaling regulates the refinement of spindle orientation in proliferative chondrocytes (Fig. 7). One possible mechanism is that Fzd signaling directly affects spindle

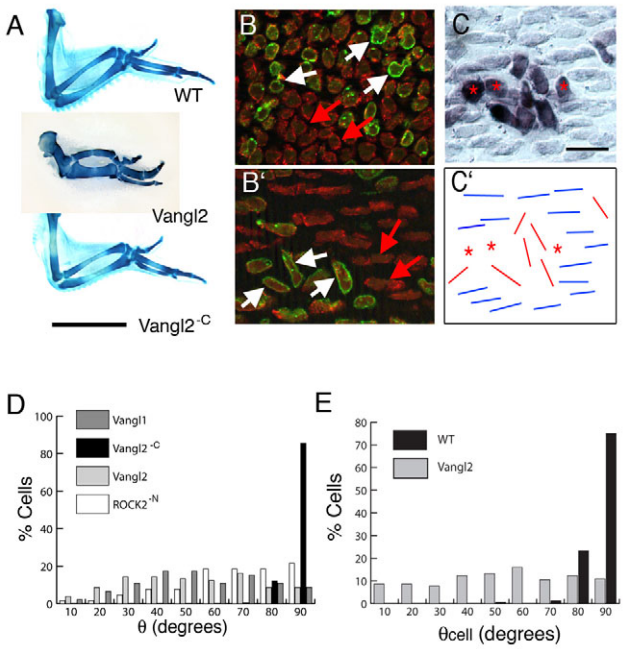

Fig. 6. Disruption of PCP signaling affects the polarity of proliferative chondrocytes. (**A**) Expression of the PCP signaling component *Vangl2*, but not the PCP-defective mutant *Vangl2*$^{-C}$, results in decreased length and increased width of chick long bones. (**B**,**B′**) Mosaic tissue expressing an epitope-tagged Vangl2 (green, white arrows) and counterstained with phalloidin (red, red arrows) shows proper secretion of the protein to the cell membrane in both resting (B) and proliferative (B′) chondrocytes. In these mosaic tissues, *Vangl2*-expressing proliferative chondrocytes exhibit defects in the orientation of the long axis, whereas *Vangl2*-expressing resting chondrocytes are normal. (**C**,**C′**) As with immunofluorescence, in situ hybridization supports the hypothesis that *Vangl2* functions cell-autonomously, as shown by the disorder of infected chondrocytes (purple in C, red bars in C′) as compared with neighboring wild-type cells (unstained cells in C, blue bars in C′). Asterisks denote cells for which a long axis could not be determined. (**D**) Expression of *Vangl2* results in a uniform distribution of telophase θ (P=0.102), whereas expression of Rock2^{-N} alters the distribution of telphase θ distinct from wild-type proliferative chondrocytes (P<0.001). Telophase θ for *Vangl1*-expressing chondrocytes is indistinguishable from that of chondrocytes expressing *Vangl2* (P=0.75). Note that the ectopic expression of either *Vangl1* or *Vangl2* produces a similar phenotype to the expression of Fzd7^{-C}, whereas the phenotype of Rock2^{-N} is weaker with respect to the orientation of the plane of cell division. Chondrocytes expressing *Vangl2*$^{-C}$ behave as wild type (P=0.4). (**E**) Quantification of the orientation of the long axis of proliferative chondrocytes shows that θ_{cell} for *Vangl2* expression is uniformly distributed from 0-90°, whereas uninfected neighboring cells display wild-type alignment. Scale bars: 500 μm in A; 50 μm in C.

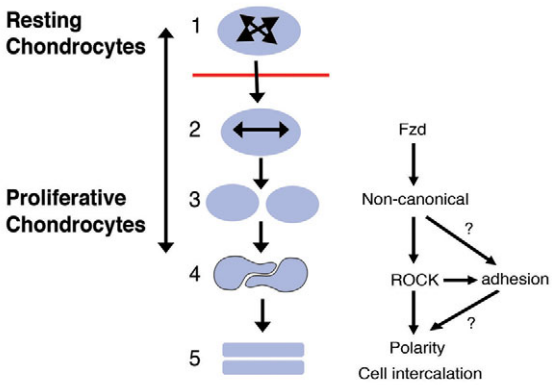

Fig. 7. Model for regulation of chondrocyte morphogenesis by Fzd signaling. Maturation of chondrocytes involves conversion from progenitor (resting) cells that divide in arbitrary planes (1, multiply oriented arrows) to proliferative chondrocytes that display aligned planes of cell division (2, bidirectional arrow). Cytokinesis in proliferative chondrocytes results in daughter cells that are initially displaced laterally relative to the column axis (3). Subsequently, these cells intercalate (4) to form a single column composed of progeny from a single progenitor cell (5). The canonical Fzd signaling pathway is important for cartilage growth and chondrogenesis, and might play a role in regulating the resting chondrocytes. However, the morphogenetic properties of proliferative chondrocytes are regulated via a noncanonical pathway. At a minimum, this pathway regulates cell polarity that is required for the proper alignment of cell divisions and orientation of the cell body. It remains to be determined whether these effects result from Fzd-dependent regulation of the extracellular matrix or cell-matrix adhesion molecules.

alignment by regulating the localization of proteins that position the centrosomes. Alternatively, noncanonical Fzd signaling might regulate cell flattening during mitosis that in turn constrains the mitotic spindle in telophase. Both models are consistent with known functions of the noncanonical pathways, but the latter model is unlikely to act predominately because the division plane is largely unchanged in *daCamKII*-expressing chondrocytes that do not flatten. That the division plane and cell shape are not tightly linked is further supported by the fact that neighboring affected cells often display different axial polarities. Instead, this suggests that, as in the neural tube (Ciruna et al., 2006), noncanonical Fzd signaling additionally functions to re-establish polarity in chondrocytes following cell division.

Re-establishing polarity after telophase might be important for column formation. Here we show by lineage analysis that following cell division newly generated daughter cells incorporate into columns in a process that is highly similar to convergent extension by cell intercalation, a coordinated cell movement that leads to the simultaneous narrowing and elongation of the anterior-posterior axis in vertebrate embryos (Elul et al., 1997; Keller et al., 1989). Daughter cells with different polarities might be unable to undergo the coordinated cell movements necessary for intercalation. However, one important difference with other examples of convergent extension is that chondrocyte columns derive from clonal expansion and not from cell recruitment, which generates mixed lineage columns in terminal filaments (TFs) of the *Drosophila* ovariole (Godt and Laski, 1995) and in the vertebrate notochord (Keller et al., 1989). In this context, noncanonical Fzd signaling might act by maintaining a functional interface between daughter cells or by promoting complementary shape changes in interacting cells.

A key question is how polarity is coordinated both locally and globally in the proliferative chondrocytes. Tissue polarity has been modeled by gradients of secreted factors or cell adhesion. A ligand-dependent signaling model is consistent with our data and the observation that *Wnt5a* functions in proliferative chondrocyte morphogenesis in mouse (Yang et al., 2003), in convergent extension movements in zebrafish (Topczewski et al., 2001; Zhu et

al., 2006), and in the polarity of stereocilia of the inner ear (Qian et al., 2007). However, it is not known whether cells determine polarity by interpreting a Wnt ligand gradient or whether Wnt signaling is required for competence to respond to other graded signals (Witze et al., 2008), and a gradient of Wnt proteins in the growth plate has not been demonstrated. One test of this model could come from understanding how heparan sulfate proteoglycans of the glypican family regulate cell intercalation via noncanonical Fzd signaling (Ohkawara et al., 2003) and from determination of whether ligand-dependent mechanisms are responsible for abnormal cartilage architecture in *Ext1* (Koziel et al., 2004) or *Gpc3* (Viviano et al., 2005) hypomorphic mice and *knypek* (*gpc4*)-null fish (Topczewski et al., 2001).

In cartilage, cell-cell contact is unlikely to globally coordinate cell polarity because cartilage structure is not altered in mature growth plates in which thick extracellular matrix separates individual columns (Dodds, 1930). Nonetheless, order within clones (columns) could result from high-fidelity adhesion-dependent local propagation of polarity initially conferred upon the mother row cell that established the column. For example, cell-cell contact through adherens junctions defines polarity in some epithelial stem cell populations (Song et al., 2002). Alternatively, cell-matrix interactions can orient matrix fibrils and determine polarized cell movement (Davidson et al., 2006; Goto and Keller, 2002; Marsden and DeSimone, 2003) via integrin receptor function (Yu et al., 2005; Yu et al., 2008; Zhou and Kramer, 2005), or provide boundary functions that promote cell intercalation (Veeman et al., 2008). A potential role for cell-matrix adhesion is further supported by altered growth plate structure in mouse mutants of cell-matrix interaction molecules (see Table S2 in the supplementary material). However, of these mutants, only loss-of-function of integrin β1 (Aszodi et al., 2003) and *ColIX* (Blumbach et al., 2008; Dreier et al., 2008) display substantial loss of proliferative chondrocyte structure. Despite similarities to the phenotypes we describe, differences such as decreased cell proliferation and hypocellularity in cell adhesion mutants suggest that the polarity defects described in the present studies might not be solely due to altered cell-matrix interactions. It remains to be determined whether Fzd signaling directly regulates integrin/matrix production or localization, or modulates integrin function by crosstalk via a Rock-dependent pathway (Fig. 7). Regardless, noncanonical Fzd signaling might help maintain cell polarity and clone identity by regulating the expression and/or localization of cell adhesion complexes on proliferative chondrocytes.

Is PCP the noncanonical pathway?

Three findings from our analysis above are consistent with the possibility that a PCP-like pathway regulates the polarity of proliferative chondrocytes. First, the similar phenotypes we observe in Fzd loss- and gain-of-function experiments are a hallmark of PCP signaling (Krasnow and Adler, 1994). Second, *Vangl* gain-of-function phenocopies *Fzd* loss-of-function, an effect that depends on the presence of the C-terminus of Vangl, which interacts with PCP proteins. Third, the cell-autonomous effects of Fzd are replicated by *D2* only when DEP function is maintained. Further support is provided by microarray analysis that shows specific regulation of the core PCP gene *Prickle1* during chondrocyte maturation (Belluoccio et al., 2008).

Although our data strongly point to a role for a PCP-like pathway in growth plate morphogenesis, direct genetic support for this model is lacking. If not the PCP pathway, which noncanonical effector pathway acts in proliferative chondrocytes? One thread that connects pathways that regulate cell polarity during convergent extension, PCP in the inner ear, and the columnar organization of proliferative chondrocytes with neurite extension (Carreira-Barbosa et al., 2003; Jessen et al., 2002; Nambiar et al., 2007) and with one specific asymmetric cell division in the *Caenorhabditis* elegans embryo (Wu and Herman, 2006b) is that each process is consistently and predictably affected by altered activity of PCP proteins. These underlying commonalities suggest the presence of a core polarity module (Lawrence et al., 2007) that regulates cytoskeletal structure via Rock activity and cell adhesion modules (Yu et al., 2005; Yu et al., 2008). Thus, context-dependent regulators might confer emergent properties on a core pathway to generate distinct mechanisms for the interpretation and propagation of cell polarity in diverse tissues.

Column formation and cartilage morphogenesis

One potential physiological role for polarized cell behaviors is the regulation of cartilage growth. In particular, cell divisions oriented to produce daughter cells aligned with the axis of growth are characteristic of growing tissues (Baena-Lopez et al., 2005; Fischer et al., 2006). Curiously, proliferative chondrocytes divide and flatten orthogonal to expectations, requiring the intercalation of daughter cells following cell division. Subsequent hypertrophy of the chondrocytes, not cell intercalation or cell proliferation, drives the elongation of cartilage (Breur et al., 1991) and of the frog notochord (Adams et al., 1990). This two-step process could ensure high-density packing of cells in the longitudinal axis to maximize the growth potential of hypertrophy while minimizing disruption of column structure during mitosis. In our studies, conditions that result in column loss produced bones that displayed decreased longitudinal growth and increased lateral expansion. Consistent with this observation, a strong correlation between long-bone dimensions and proliferative chondrocyte structure exists in the literature (Aszodi et al., 2003; Blumbach et al., 2008; Dreier et al., 2008; Viviano et al., 2005; Yang et al., 2003). Thus, chondrocyte columns appear to orient vectors of growth and, therefore, regulated cell polarity could provide vertebrates with a powerful system for sculpting the diverse morphologies of bone that are required to generate an articulated skeleton.

We thank Linda Chee for generating retroviruses; Chen-Ming Chuong, Phillipa Francis-West, Matsuhiro Iwamoto, Carole LaBonne, Ray Keller, Randall Moon, Clifford Tabin and John Wallingford for plasmids; Hongmei Jiang for statistical analysis; and Molly Ahrens, Greg Beitel, Richard Carthew and Robert Holmgren for comments and discussion. This work was supported by funding from the Searle Leadership Fund of the Chicago Community Trust, the Alumnae of Northwestern University, the National Center for Research Resources (NCRR 1C06RR015497-01), and the National Institutes of Health (NIAMS AR054857-01). The authors state that there are no conflicts of interest. Deposited in PMC for release after 12 months.

Supplementary material

Supplementary material for this article is available at http://dev.biologists.org/cgi/content/full/136/7/1083/DC1

References

Abad, V., Meyers, J. L., Weise, M., Gafni, R. I., Barnes, K. M., Nilsson, O., Bacher, J. D. and Baron, J. (2002). The role of the resting zone in growth plate chondrogenesis. *Endocrinology* **143**, 1851-1857.

Abzhanov, A., Kuo, W. P., Hartmann, C., Grant, B. R., Grant, P. R. and Tabin, C. J. (2006). The calmodulin pathway and evolution of elongated beak morphology in Darwin's finches. *Nature* **442**, 563-567.

Adams, D. S., Keller, R. and Koehl, M. A. (1990). The mechanics of notochord elongation, straightening and stiffening in the embryo of Xenopus laevis. *Development* **110**, 115-130.

Adler, P. N. and Taylor, J. (2001). Asymmetric cell division: plane but not simple. *Curr. Biol.* **11**, R233-R236.

Alvarez, J., Horton, J., Sohn, P. and Serra, R. (2001). The perichondrium plays an important role in mediating the effects of TGF-beta1 on endochondral bone formation. *Dev. Dyn.* **221**, 311-321.
Aszodi, A., Hunziker, E. B., Brakebusch, C. and Fassler, R. (2003). Beta1 integrins regulate chondrocyte rotation, G1 progression, and cytokinesis. *Genes Dev.* **17**, 2465-2479.
Axelrod, J. D., Miller, J. R., Shulman, J. M., Moon, R. T. and Perrimon, N. (1998). Differential recruitment of Dishevelled provides signaling specificity in the planar cell polarity and Wingless signaling pathways. *Genes Dev.* **12**, 2610-2622.
Baena-Lopez, L. A., Baonza, A. and Garcia-Bellido, A. (2005). The orientation of cell divisions determines the shape of Drosophila organs. *Curr. Biol.* **15**, 1640-1644.
Belluoccio, D., Bernardo, B. C., Rowley, L. and Bateman, J. F. (2008). A microarray approach for comparative expression profiling of the discrete maturation zones of mouse growth plate cartilage. *Biochim. Biophys. Acta* **1779**, 330-340.
Blumbach, K., Niehoff, A., Paulsson, M. and Zaucke, F. (2008). Ablation of collagen IX and COMP disrupts epiphyseal cartilage architecture. *Matrix Biol.* **27**, 306-318.
Boutros, M., Paricio, N., Strutt, D. I. and Mlodzik, M. (1998). Dishevelled activates JNK and discriminates between JNK pathways in planar polarity and wingless signaling. *Cell* **94**, 109-118.
Breur, G. J., VanEnkevort, B. A., Farnum, C. E. and Wilsman, N. J. (1991). Linear relationship between the volume of hypertrophic chondrocytes and the rate of longitudinal bone growth in growth plates. *J. Orthop. Res.* **9**, 348-359.
Carreira-Barbosa, F., Concha, M. L., Takeuchi, M., Ueno, N., Wilson, S. W. and Tada, M. (2003). Prickle 1 regulates cell movements during gastrulation and neuronal migration in zebrafish. *Development* **130**, 4037-4046.
Chen, C. M., Smith, D. M., Peters, M. A., Samson, M. E., Zitz, J., Tabin, C. J. and Cepko, C. L. (1999). Production and design of more effective avian replication-incompetent retroviral vectors. *Dev. Biol.* **214**, 370-384.
Ciruna, B., Jenny, A., Lee, D., Mlodzik, M. and Schier, A. F. (2006). Planar cell polarity signalling couples cell division and morphogenesis during neurulation. *Nature* **439**, 220-224.
Cottrill, C. P., Archer, C. W. and Wolpert, L. (1987). Cell sorting and chondrogenic aggregate formation in micromass culture. *Dev. Biol.* **122**, 503-515.
Davidson, L. A., Marsden, M., Keller, R. and Desimone, D. W. (2006). Integrin alpha5beta1 and fibronectin regulate polarized cell protrusions required for Xenopus convergence and extension. *Curr. Biol.* **16**, 833-844.
Dodds, G. (1930). Row formation and other types of arrangement of cartilage cells in endochondral ossification. *Anat. Rec.* **46**, 385-399.
Dreier, R., Opolka, A., Grifka, J., Bruckner, P. and Grassel, S. (2008). Collagen IX-deficiency seriously compromises growth cartilage development in mice. *Matrix Biol.* **27**, 319-329.
Elul, T., Koehl, M. A. and Keller, R. (1997). Cellular mechanism underlying neural convergent extension in Xenopus laevis embryos. *Dev. Biol.* **191**, 243-258.
Fischer, E., Legue, E., Doyen, A., Nato, F., Nicolas, J. F., Torres, V., Yaniv, M. and Pontoglio, M. (2006). Defective planar cell polarity in polycystic kidney disease. *Nat. Genet.* **38**, 21-23.
Godt, D. and Laski, F. A. (1995). Mechanisms of cell rearrangement and cell recruitment in Drosophila ovary morphogenesis and the requirement of bric a brac. *Development* **121**, 173-187.
Gong, Y., Mo, C. and Fraser, S. E. (2004). Planar cell polarity signalling controls cell division orientation during zebrafish gastrulation. *Nature* **430**, 689-693.
Goto, T. and Keller, R. (2002). The planar cell polarity gene strabismus regulates convergence and extension and neural fold closure in Xenopus. *Dev. Biol.* **247**, 165-181.
Ham, A. W. (1932). The variability of the planes of cell division in the cartilage columns of the growing epiphyseal plate. *Anat. Rec.* **51**, 125-133.
Hamburger, V. and Hamilton, H. L. (1992). A series of normal stages in the development of the chick embryo. 1951. *Dev. Dyn.* **195**, 231-272.
Hartmann, C. and Tabin, C. J. (2000). Dual roles of Wnt signaling during chondrogenesis in the chicken limb. *Development* **127**, 3141-3159.
Herrick, R. M. (1965). A short-cut solution for the Kolmogorov-Smirnov test. NADC-MR-6504. *NADC-MR Rep*. 1-4.
Hill, T. P., Spater, D., Taketo, M. M., Birchmeier, W. and Hartmann, C. (2005). Canonical Wnt/beta-catenin signaling prevents osteoblasts from differentiating into chondrocytes. *Dev. Cell* **8**, 727-738.
Hinoi, E., Bialek, P., Chen, Y. T., Rached, M. T., Groner, Y., Behringer, R. R., Ornitz, D. M. and Karsenty, G. (2006). Runx2 inhibits chondrocyte proliferation and hypertrophy through its expression in the perichondrium. *Genes Dev.* **20**, 2937-2942.
Hughes, S. H. (2004). The RCAS vector system. *Folia Biol. (Praha)* **50**, 107-119.
Hunziker, E. B., Schenk, R. K. and Cruz-Orive, L. M. (1987). Quantitation of chondrocyte performance in growth-plate cartilage during longitudinal bone growth. *J. Bone Joint Surg. Am.* **69**, 162-173.
Jessen, J. R., Topczewski, J., Bingham, S., Sepich, D. S., Marlow, F., Chandrasekhar, A. and Solnica-Krezel, L. (2002). Zebrafish trilobite identifies new roles for Strabismus in gastrulation and neuronal movements. *Nat. Cell Biol.* **4**, 610-615.
Keller, R., Cooper, M. S., Danilchik, M., Tibbetts, P. and Wilson, P. A. (1989). Cell intercalation during notochord development in Xenopus laevis. *J. Exp. Zool.* **251**, 134-154.
Keller, R., Davidson, L., Edlund, A., Elul, T., Ezin, M., Shook, D. and Skoglund, P. (2000). Mechanisms of convergence and extension by cell intercalation. *Philos. Trans. R. Soc. Lond. B Biol. Sci.* **355**, 897-922.
Kengaku, M., Capdevila, J., Rodriguez-Esteban, C., De La Pena, J., Johnson, R. L., Belmonte, J. C. and Tabin, C. J. (1998). Distinct WNT pathways regulating AER formation and dorsoventral polarity in the chick limb bud. *Science* **280**, 1274-1277.
Kim, G. H. and Han, J. K. (2005). JNK and ROKalpha function in the noncanonical Wnt/RhoA signaling pathway to regulate Xenopus convergent extension movements. *Dev. Dyn.* **232**, 958-968.
Klein, T. J. and Mlodzik, M. (2005). Planar cell polarization: an emerging model points in the right direction. *Annu. Rev. Cell Dev. Biol.* **21**, 155-176.
Koziel, L., Kunath, M., Kelly, O. G. and Vortkamp, A. (2004). Ext1-dependent heparan sulfate regulates the range of Ihh signaling during endochondral ossification. *Dev. Cell* **6**, 801-813.
Krasnow, R. E. and Adler, P. N. (1994). A single frizzled protein has a dual function in tissue polarity. *Development* **120**, 1883-1893.
Kronenberg, H. M. (2003). Developmental regulation of the growth plate. *Nature* **423**, 332-336.
Kuhl, M., Sheldahl, L. C., Malbon, C. C. and Moon, R. T. (2000). Ca(2+)/calmodulin-dependent protein kinase II is stimulated by Wnt and Frizzled homologs and promotes ventral cell fates in Xenopus. *J. Biol. Chem.* **275**, 12701-12711.
Lawrence, P. A., Struhl, G. and Casal, J. (2007). Planar cell polarity: one or two pathways? *Nat. Rev. Genet.* **8**, 555-563.
Leung, T., Chen, X. Q., Manser, E. and Lim, L. (1996). The p160 RhoA-binding kinase ROK alpha is a member of a kinase family and is involved in the reorganization of the cytoskeleton. *Mol. Cell. Biol.* **16**, 5313-5327.
Logan, M. and Tabin, C. (1998). Targeted gene misexpression in chick limb buds using avian replication-competent retroviruses. *Methods* **14**, 407-420.
Mak, K. K., Chen, M. H., Day, T. F., Chuang, P. T. and Yang, Y. (2006). Wnt/beta-catenin signaling interacts differentially with Ihh signaling in controlling endochondral bone and synovial joint formation. *Development* **133**, 3695-3707.
Marsden, M. and DeSimone, D. W. (2003). Integrin-ECM interactions regulate cadherin-dependent cell adhesion and are required for convergent extension in Xenopus. *Curr. Biol.* **13**, 1182-1191.
Nambiar, R. M., Ignatius, M. S. and Henion, P. D. (2007). Zebrafish colgate/hdac1 functions in the non-canonical Wnt pathway during axial extension and in Wnt-independent branchiomotor neuron migration. *Mech. Dev.* **124**, 682-698.
Nasevicius, A., Hyatt, T., Kim, H., Guttman, J., Walsh, E., Sumanas, S., Wang, Y. and Ekker, S. C. (1998). Evidence for a frizzled-mediated wnt pathway required for zebrafish dorsal mesoderm formation. *Development* **125**, 4283-4292.
Ohkawara, B., Yamamoto, T. S., Tada, M. and Ueno, N. (2003). Role of glypican 4 in the regulation of convergent extension movements during gastrulation in Xenopus laevis. *Development* **130**, 2129-2138.
Ong, L. D. and LeClare, P. C. (1968). The Kolmogorov-Smirnov test for the log-normality of sample cumulative frequency distributions. *Health Phys.* **14**, 376.
Papkoff, J., Rubinfeld, B., Schryver, B. and Polakis, P. (1996). Wnt-1 regulates free pools of catenins and stabilizes APC-catenin complexes. *Mol. Cell. Biol.* **16**, 2128-2134.
Park, M. and Moon, R. T. (2002). The planar cell-polarity gene stbm regulates cell behaviour and cell fate in vertebrate embryos. *Nat. Cell Biol.* **4**, 20-25.
Phillips, H. M., Murdoch, J. N., Chaudhry, B., Copp, A. J. and Henderson, D. J. (2005). Vangl2 acts via RhoA signaling to regulate polarized cell movements during development of the proximal outflow tract. *Circ. Res.* **96**, 292-299.
Qian, D., Jones, C., Rzadzinska, A., Mark, S., Zhang, X., Steel, K. P., Dai, X. and Chen, P. (2007). Wnt5a functions in planar cell polarity regulation in mice. *Dev. Biol.* **306**, 121-133.
Roegiers, F., Younger-Shepherd, S., Jan, L. Y. and Jan, Y. N. (2001). Two types of asymmetric divisions in the Drosophila sensory organ precursor cell lineage. *Nat. Cell Biol.* **3**, 58-67.
Rothbacher, U., Laurent, M. N., Deardorff, M. A., Klein, P. S., Cho, K. W. and Fraser, S. E. (2000). Dishevelled phosphorylation, subcellular localization and multimerization regulate its role in early embryogenesis. *EMBO J.* **19**, 1010-1022.
Rubinfeld, B., Robbins, P., El-Gamil, M., Albert, I., Porfiri, E. and Polakis, P. (1997). Stabilization of beta-catenin by genetic defects in melanoma cell lines. *Science* **275**, 1790-1792.
Song, X., Zhu, C. H., Doan, C. and Xie, T. (2002). Germline stem cells anchored by adherens junctions in the Drosophila ovary niches. *Science* **296**, 1855-1857.

Suksaweang, S., Lin, C. M., Jiang, T. X., Hughes, M. W., Widelitz, R. B. and Chuong, C. M. (2004). Morphogenesis of chicken liver: identification of localized growth zones and the role of beta-catenin/Wnt in size regulation. *Dev. Biol.* **266**, 109-122.

Tibber, M. S., Kralj-Hans, I., Savage, J., Mobbs, P. G. and Jeffery, G. (2004). The orientation and dynamics of cell division within the plane of the developing vertebrate retina. *Eur. J. Neurosci.* **19**, 497-504.

Topczewski, J., Sepich, D. S., Myers, D. C., Walker, C., Amores, A., Lele, Z., Hammerschmidt, M., Postlethwait, J. and Solnica-Krezel, L. (2001). The zebrafish glypican knypek controls cell polarity during gastrulation movements of convergent extension. *Dev. Cell* **1**, 251-264.

Toyoshima, F. and Nishida, E. (2007). Integrin-mediated adhesion orients the spindle parallel to the substratum in an EB1- and myosin X-dependent manner. *EMBO J.* **26**, 1487-1498.

Tufan, A. C., Daumer, K. M. and Tuan, R. S. (2002). Frizzled-7 and limb mesenchymal chondrogenesis: effect of misexpression and involvement of N-cadherin. *Dev. Dyn.* **223**, 241-253.

Veeman, M. T., Nakatani, Y., Hendrickson, C., Ericson, V., Lin, C. and Smith, W. C. (2008). Chongmague reveals an essential role for laminin-mediated boundary formation in chordate convergence and extension movements. *Development* **135**, 33-41.

Viviano, B. L., Silverstein, L., Pflederer, C., Paine-Saunders, S., Mills, K. and Saunders, S. (2005). Altered hematopoiesis in glypican-3-deficient mice results in decreased osteoclast differentiation and a delay in endochondral ossification. *Dev. Biol.* **282**, 152-162.

Wallingford, J. B. and Harland, R. M. (2002). Neural tube closure requires Dishevelled-dependent convergent extension of the midline. *Development* **129**, 5815-5825.

Wallingford, J. B. and Habas, R. (2005). The developmental biology of Dishevelled: an enigmatic protein governing cell fate and cell polarity. *Development* **132**, 4421-4436.

Wallingford, J. B., Rowning, B. A., Vogeli, K. M., Rothbacher, U., Fraser, S. E. and Harland, R. M. (2000). Dishevelled controls cell polarity during Xenopus gastrulation. *Nature* **405**, 81-85.

Wilson, E. B. (1900). *The Cell in Development and Inheritance*. Norwood, MA: The Macmillian Company, Norwood Press.

Witze, E. S., Litman, E. S., Argast, G. M., Moon, R. T. and Ahn, N. G. (2008). Wnt5a control of cell polarity and directional movement by polarized redistribution of adhesion receptors. *Science* **320**, 365-369.

Wu, M. and Herman, M. A. (2006a). A novel noncanonical Wnt pathway is involved in the regulation of the asymmetric B cell division in C. elegans. *Dev. Biol.* **293**, 316-329.

Wu, M. and Herman, M. A. (2006b). Asymmetric localizations of LIN-17/Fz and MIG-5/Dsh are involved in the asymmetric B cell division in C. elegans. *Dev. Biol.* **303**, 650-662.

Yang, Y., Topol, L., Lee, H. and Wu, J. (2003). Wnt5a and Wnt5b exhibit distinct activities in coordinating chondrocyte proliferation and differentiation. *Development* **130**, 1003-1015.

Yu, W., Datta, A., Leroy, P., O'Brien, L. E., Mak, G., Jou, T. S., Matlin, K. S., Mostov, K. E. and Zegers, M. M. (2005). Beta1-integrin orients epithelial polarity via Rac1 and laminin. *Mol. Biol. Cell* **16**, 433-445.

Yu, W., Shewan, A. M., Brakeman, P., Eastburn, D. J., Datta, A., Bryant, D. M., Fan, Q. W., Weiss, W. A., Zegers, M. M. and Mostov, K. E. (2008). Involvement of RhoA, ROCK I and myosin II in inverted orientation of epithelial polarity. *EMBO Rep.* **9**, 923-929.

Zhou, H. and Kramer, R. H. (2005). Integrin engagement differentially modulates epithelial cell motility by RhoA/ROCK and PAK1. *J. Biol. Chem.* **280**, 10624-10635.

Zhu, S., Liu, L., Korzh, V., Gong, Z. and Low, B. C. (2006). RhoA acts downstream of Wnt5 and Wnt11 to regulate convergence and extension movements by involving effectors Rho kinase and Diaphanous: use of zebrafish as an in vivo model for GTPase signaling. *Cell Signal.* **18**, 359-372.